Publications

Available Online

J. Sci. Res. **13** (3), 891-900 (2021)

JOURNAL OF SCIENTIFIC RESEARCH

www.banglajol.info/index.php/JSR

The Optical Properties of Dy^{3+} Doped $LaPO_4$ Phosphors Prepared by Solid State Reaction Method

C. A. Rao[1*], K. Shakampally[2], K. V. R. Murthy[3]

[1]Department of Physics, Bapatla College of Arts & Sciences, Bapatla - 522101, A. P, India

[2]Department of Physics, Nalla Malla Reddy Engineering College, Ranga Reddy District-500088, Telangana, India

[3]Display Materials Laboratory, Applied Physics Department, Faculty of Technology and Engineering, M. S. University of Baroda, Vadodara-390001, India

Received 2 May 2021, accepted in final revised form 10 July 2021

Abstract

Luminescent nanomaterials are used in everyday life due to their employment in distinct fields of science and technology, like cathode ray tubes (CRTs), flat panel display devices, temperature sensors, lasers, solar-cells, biological imaging, and solid-state lighting but also as carriers for miscellaneous therapeutic drugs. We have prepared dysprosium Dy^{3+} (0.5 mol %) doped lanthanum phosphate ($LaPO_4$) phosphor by solid state reaction method. The excitation spectra of synthesized phosphor at 595 nm monitoring were composed of broadband and a series of sharp peaks, the strongest excitation peak at 254, 271, and 350 nm. The main emission spectra of samples under 254, 271, and 350 nm excitation are Dy^{3+} (0.5 mol %) doped $LaPO_4$ phosphor observed at 477 and 573 nm corresponding to blue and yellow color. The broadband emission is the characteristic of the allowed f-h transition of Dy^{3+} ions. The corresponding emission band is observed due to the (blue emission) $^4f_{9/2}\rightarrow{}^6h_{15/2}$, (yellow emission) $^4f_{9/2}\rightarrow{}^6h_{13/2}$ transition of Dy^{3+} ions. All the samples have been characterized by X-ray powder diffraction (XRD), scanning electron microscopy (SEM), Fourier transform infrared spectroscopy (FTIR), and photoluminescence (PL) techniques.

Keywords: Lanthanum phosphate ($LaPO_4$) phosphor; Dysprosium (Dy^{3+}) ion; Solid state reaction.

doi: http://dx.doi.org/10.3329/jsr.v13i3.53287 J. Sci. Res. **13** (3), 891-900 (2021)

1. Introduction

Nowadays, research on the synthesis of inorganic luminescent material with proper dimensions and morphologies has attracted great attention. Inorganic luminescent materials like lanthanum phosphate ($LaPO_4$) have found many practical applications in the field of electroluminescent devices, integrated optics, biological labels, modern lighting, and display fields [1,2]. Among different lanthanide phosphates (or) lanthanide orthophosphates ($LnPO_4$) systems, $LaPO_4$ is perhaps the most studied one, in particular,

[*]*Corresponding author*: atchyyuth@gmail.com

its monoclinic polymorph (monazite). This material has been suggested as a good candidate for the immobilization of radioactive waste elements and protective coating for ceramics [3,4]. Besides, it is one of the most commonly employed host matrices for the preparation of lanthanide-based phosphors. The production and marketing of cost-effective, energy-saving, and size-reduced nanomaterials with different shapes are of major importance for the development of multifunctional optical, magnetic, and electrical properties and functions and to unfold new domains of theoretical and technological importance [5,6]. It is well known that the optical properties of luminescent materials depend on the properties of the host material and the electronic structure and the concentration of the rare-earth ions. In nanomaterials, optical properties are also influenced by the size and morphology of particles, generally showing reduced quantum efficiency of emission in small-size particles [7-9]. The fluorescent materials with tuned emission in the visible region and promising applications as bio-labels are obtained when monazite nanoparticles are doped with some lanthanide (Ln) cations such as Eu, Ce, Tb, or Dy. $LaPO_4$ possesses the properties like low solubility in water, very high thermal stability, and high refractive index. Because of these properties, it has got importance for the production of display lamps and sensors. Dysprosium (Dy^{3+}) doped $LaPO_4$ materials have potential applications in fluorescent lamps, optoelectronics, and telecommunication [10-12]. Different methods can be used to synthesize lanthanide phosphate like solid state reaction, combustion, sol-gel, hydrothermal, precipitation, micro-emulsion, etc. [13-15]. In the present work, the prepared dysprosium Dy^{3+} (0.5 mol %) doped $LaPO_4$ phosphor is synthesized by solid state reaction method fired at 1200 ℃ for 3h. The prepared sample was analyzed by XRD, SEM, FTIR, and PL measurement.

2. Materials and Methods

2.1. *Materials preparation*

All the chemical reagents used in this experiment were analytical reagent (AR) grade pure and used without further purification. Lanthanum oxide (La_2O_3) (Sigma-Aldrich Chemie, Inc, Germany) was used as a host material. Ammonium dihydrogen phosphate ($NH_4.H_2PO_4$) (Sigma-Aldrich Chemie, Inc, Germany) was used as precipitating agent and catalyst. Dysprosium oxide (Dy_2O_3) (National Chemicals, Nutan Gujarat Industrial Estate, Vadodara, India) was used as a dopant, and almost all chemicals of assay 99.999 % were used. The stoichiometric mixture of these starting materials of powders was thoroughly grounded into homogenized using an agate motor and pestle for 1h, then put into an alumina crucible and heated at 1200 °C for 3 h with a heating rate of 5 °C/min in the muffle furnace. Finally, the samples were allowed to cool down to room temperature for about 20 h. The prepared sample powders were again grounded into homogenized using an agate motor and pestle for 10min for characteristic measurements [16,17].

2.2. *Analysis method*

This synthesis route is very easy and does not require expensive as well as sophisticated equipment. The major advantage of the solid state reaction (SSR) method is that the final product in solid form is structurally pure with the desired properties depending on the final sintering temperatures. This method is environmentally eco-friendly, and no toxic or unwanted waste is produced after the SSR method is completed. In this process, the powders produced from SSR method are very fine, and the cross-contamination is very little. This method is also very convenient for large-scale production on an industrial scale. Several complementary methods were used to characterize the prepared phosphors. To identify the crystal phase, X-ray diffraction (XRD) analysis was carried out with a powder X-ray diffractometer (Indus beam line-II (ADXRD BL-12), RRCAT, Indore, India). The electron source size at this port is approximately 0.5 mm (H) × 0.5 mm (v). The beam acceptance of the beam line is 2mrad (H) X 0.2mrad (V). The morphologies (scanning electron microscope, SEM) of the phosphor powders were obtained by using the Nova NanoSEM450 (CIU-Lab-Central University, Hyderabad). The scanning time was 10 s and 2θ ranges from 15 to 60°. The photoluminescence (PL) emission spectra were measured by a spectrofluorophotometer (SHIMADZU, RF-5301 PC) using a xenon lamp as an excitation source (MSU-Vadodara, Department of Applied Physics). All the spectra were recorded at room temperature. Emission and excitation spectra were recorded using a spectral slit width of 1.5 nm [18,19].

3. Results and Discussion

3.1. *Phase identification and crystal structure*

The phase identification, crystal structure, purity of the prepared powder samples of $LaPO_4$ phosphors, and dysprosium (Dy^{3+}) (0.5 mol %) doped $LaPO_4$ phosphors were detected by XRD. Fig. 1 represents the XRD patterns of pure $LaPO_4$ phosphors. It shows that all the diffraction peaks are in good agreement with the standard data of $LaPO_4$ (JCPDS card No. 32−0493), and no impurity peak was detected, indicating the prepared samples as single phase. According to the XRD patterns of pure $LaPO_4$ phosphors, it can be seen from the pattern that all the samples exhibit the characteristic diffractions of crystalline monoclinic $LaPO_4$. No traces of impurity phases were observed in the XRD patterns of $LaPO_4$ phosphors. The average crystallite size of 28 nm was calculated for pure $LaPO_4$ phosphor by using Debye-Scherer's formula.

$$D = K.\lambda/\beta \cos\theta \text{----------} \quad (1)$$

Where K = 0.94, D represents the crystallite size (Å), λ is the wavelength of CuKα radiation, and β is the corrected half-width at full maxima (HWFM) of the diffraction peak. Unit cell volume decreases with Dy^{3+} (0.5 mol %) doped $LaPO_4$ phosphor indicating homogeneous substitution of La^{3+} ions in $LaPO_4$ by Dy^{3+}. The XRD patterns of Dy^{3+} (0.5 mol %) doped $LaPO_4$ phosphor has been depicted in Fig. 2. It is observed that the crystallite sizes of Dy^{3+} (0.5 mol %) doped $LaPO_4$ phosphor are found to be decreased to

16 nm. It is also observed that no change in peak positions, but the intensity of the main peak is increased by 10 %, maybe for purity and complete single phase.

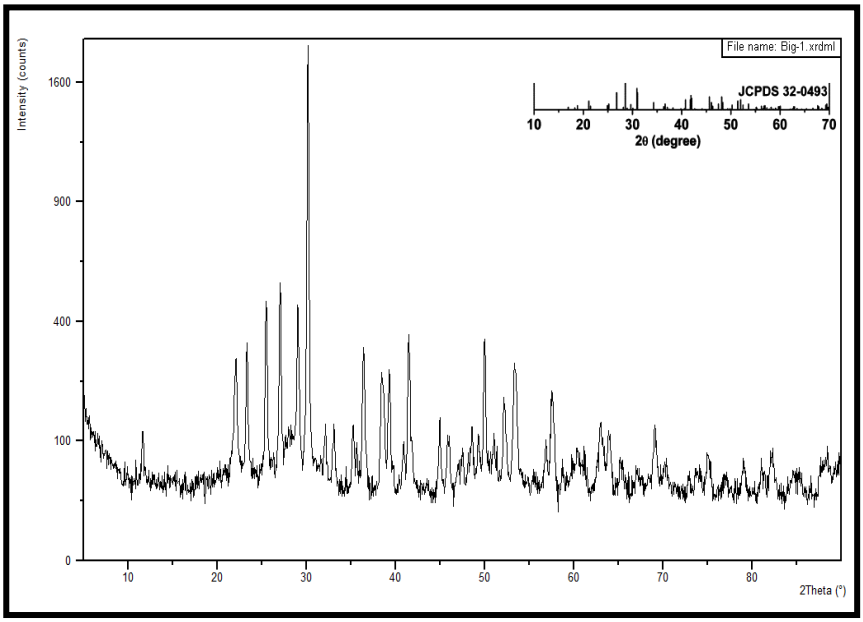

Fig.1. XRD patterns of pure $LaPO_4$ phosphor.

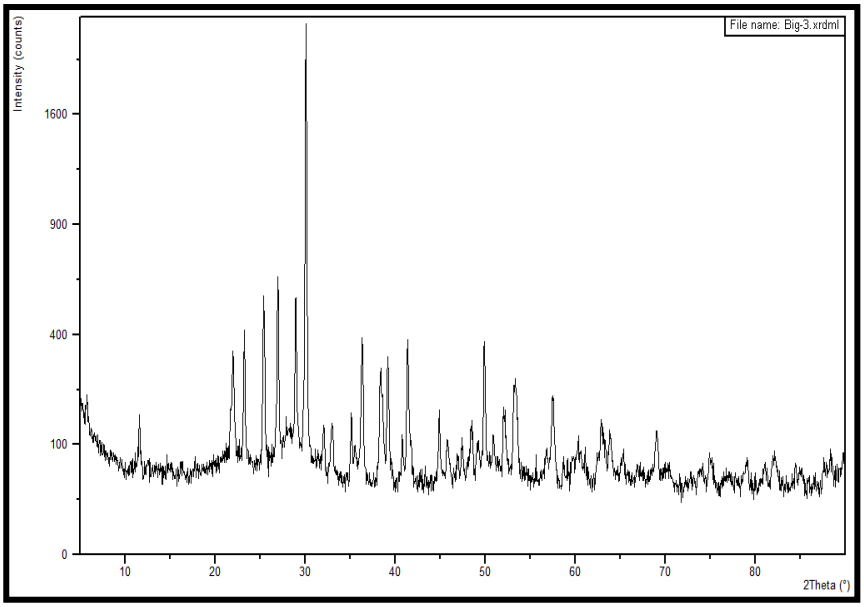

Fig.2. XRD patterns of Dy^{3+} (0.5 mol %) doped $LaPO_4$ phosphor.

3.2. *SEM morphology*

The SEM morphology micrograph images of pure and Dy^{3+} (0.5 mol %) doped $LaPO_4$ phosphor are as shown in Figs. 3(a) and 3(b). From the SEM images, it can be seen clearly that the structure of synthesized phosphor has different sizes and irregular shapes of bunching of flowers with different resolutions. The average size of particles of pure $LaPO_4$ phosphor is around 10µm. Incorporating Dy^{3+} (0.5 mol %) doped $LaPO_4$ phosphor reveals the reduction of the size particles to about 2µm. The examined SEM micrograph shows that the pure and Dy^{3+} (0.5 mol %) doped $LaPO_4$ phosphor samples originated from the solid microcrystalline structure with some agglomeration between the grains. The grains appeared agglomerated owing to the high-temperature solid-state synthesis. These phosphors can be very easily employed in lighting display technology and various coating display illuminating applications. The overall SEM studies concluding us the phosphors can be grounded mechanically and sieved to get the uniform size to use as phosphors in devices like compact fluorescent lamps (CFL) and fluorescent lamps [FL] [20,21].

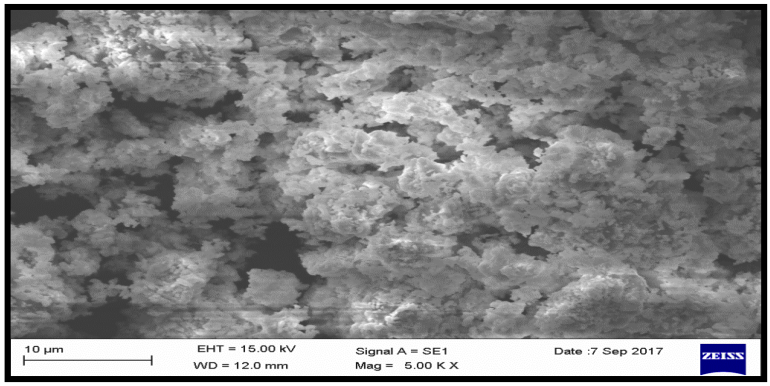

Fig. 3(a). SEM micrograph of pure $LaPO_4$ phosphor.

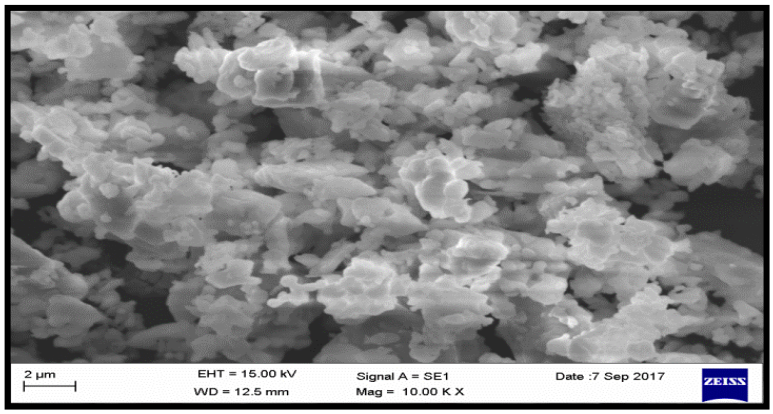

Fig. 3(b). SEM micrograph of Dy^{3+} (0.5 mol %) doped $LaPO_4$ phosphor.

3.3. *FTIR study*

FTIR spectrum is one of the most common spectroscopic techniques used by organic and inorganic compounds. The FTIR technique is to count the absorption of various infrared radiations by the target material, to develop an IR spectrum that can recognize functional groups and molecular structure in the sample. The FTIR spectra were recorded within the wave number range 4000 to 500 cm^{-1} on (Jasco-4100) FTIR spectrometerinstrument. Fig. 4 shows the FTIR spectrum of dysprosium (Dy^{3+}) (0.5 mol %) doped $LaPO_4$ phosphor. A large band is also observed at 1450 cm^{-1} and is assigned to the phosphate group PO_4^{3-} in υ_3 region anti-symmetric stretching of the P–O band. It is also observed that the peaks located at 530, 697, 860, and 1067 cm^{-1} are due to υ_4 regional vibration of PO_4^{3-}groups [22,23]. The peaks at 3467 cm^{-1} are observed due to the bending stretch vibration of the O–H group of capping agent PEG near the standing stretching of the O-H group.

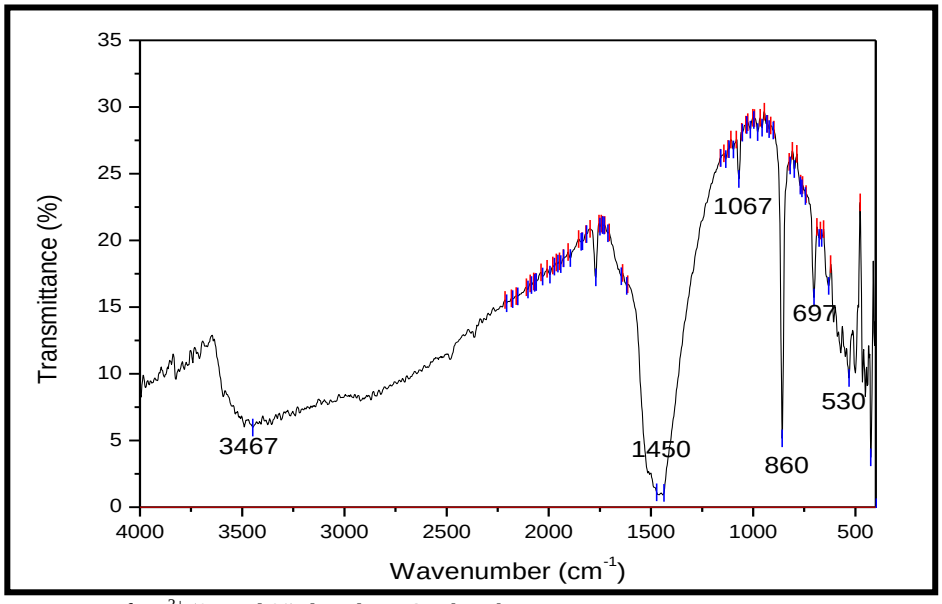

Fig. 4. FTIR of Dy^{3+} (0.5mol %) doped $LaPO_4$ phosphor.

3.4. *Luminescence properties of Dy^{3+} doped materials*

The PL excitation and emission spectrum of dysprosium (Dy^{3+}) (0.5 mol %) doped $LaPO_4$ phosphor under different excitations are as shown in Fig. 5. The excitation and emission spectra of Dy^{3+} (0.5 mol %) doped $LaPO_4$ phosphor at 595 nm monitoring were composed of broadband and a series of sharp peaks at 254, 271, and 350 nm. From the emission spectra of Dy^{3+} (0.5 mol %) doped $LaPO_4$ phosphor is observed at 477 and 573 nm, corresponding to blue and yellow color when monitored at excitation wavelength 254 and 350 nm. The broadband emission is the characteristic of the allowed H–F transition of 251 Dy^{3+} ions [24]. The corresponding emission band is observed due to the (blue emission)

$^4F_{9/2} \rightarrow {}^6H_{15/2}$, (yellow emission) $^4F_{9/2} \rightarrow {}^6H_{13/2}$ transitions of Dy^{3+} ions are well resolved with sufficient temperature. Dy^{3+} (0.5 mol %) doped $LaPO_4$ phosphor under different excitations are synthesized by solid state reaction method; favorable emission in the deep blue region is one of the best candidates as blue light-emitting phosphors and are suitable for SSL technological applications in the LED devices [25-28].

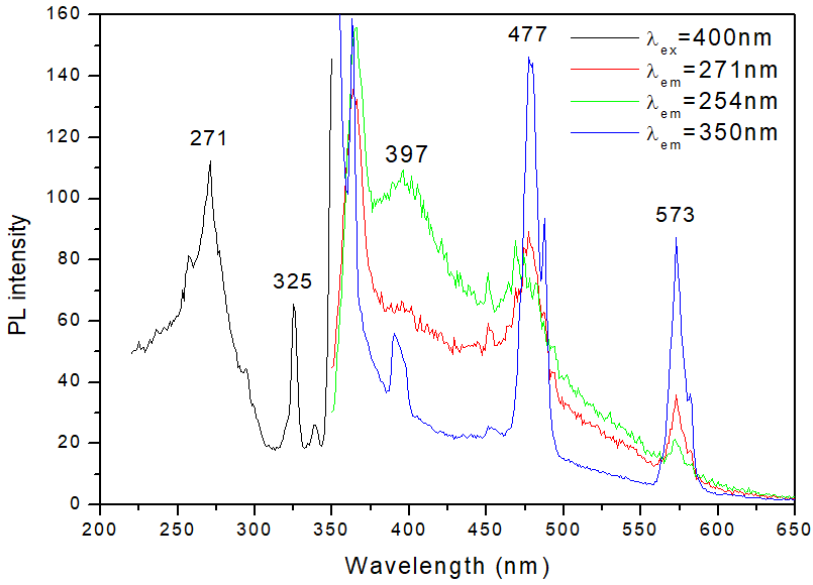

Fig. 5. Excitation and emission spectrum of Dy^{3+} (0.5 mol %) doped $LaPO_4$ phosphor under different excitations.

3.5. *CIE analysis*

The CIE coordinates were calculated by the spectrophotometric method using the spectral energy distribution. The luminescence color coordinates of dysprosium (Dy^{3+}) (0.5 mol %) doped $LaPO_4$ phosphor under different excitations have been characterized by the CIE (commission international de I'Eclairage) 1931-color chart chromaticity diagram [29]. Fig. 6 shows the color coordinates emission spectrum of the dysprosium (Dy^{3+}) (0.5 mol %) doped $LaPO_4$ phosphor converted to the CIE 1931-color chart chromaticity using the CIE software from Radiant Imaging. Points (A) are x = 0.142 and y = 0.087 indicating to blue color (λ_{em}= 477 nm), and Points (B) are X=0.425 and Y=0.511 indicating to yellow color (λ_{em}= 573 nm) under 254 and 350 nm excitation wavelengths.

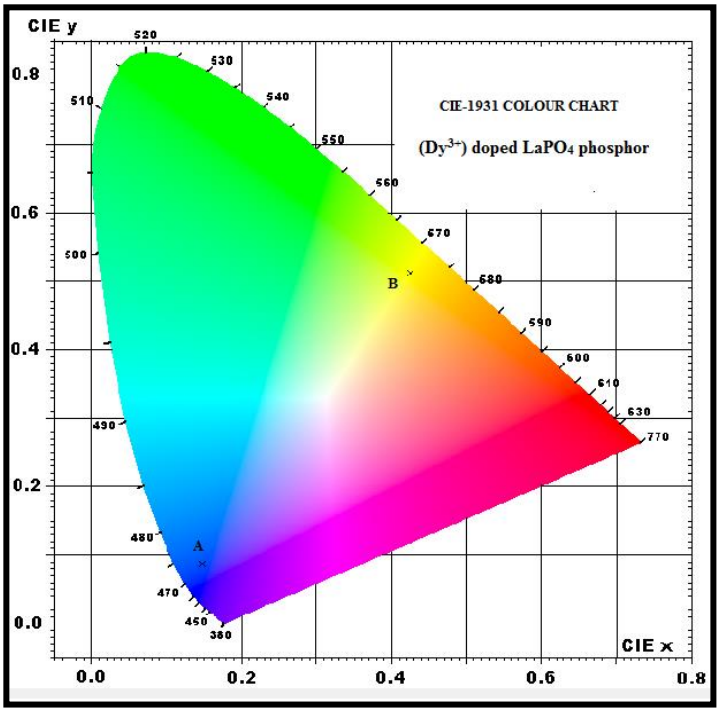

Fig. 6. CIE coordinates of (Dy^{3+}) doped $LaPO_4$ phosphor.

4. Conclusion

In summary, novel Dy^{3+} (0.5 mol %) doped $LaPO_4$ phosphors have been successfully synthesized by SSR method at high temperatures. The phase identification, surface morphology, and spectroscopic techniques of pure and Dy^{3+} (0.5 mol %) doped $LaPO_4$ phosphors have been identified by the XRD, SEM, and FTIR, respectively.

Photoluminescence emission spectra of prepared materials showed intense blue and yellow color with 254, 350 nm excitation. The strong intense peak of these light-emitting materials was located in 477 and 573 nm regions due to (blue emission) $^4F_{9/2} \rightarrow {}^6H_{15/2}$, (yellow emission) $^4F_{9/2} \rightarrow {}^6H_{13/2}$ transitions of Dy^{3+} ions. The maximum luminescence intensity of the phosphors was obtained when these materials were heated at 1200 °C.

According to the XRD patterns, the average crystallite size was calculated for pure $LaPO_4$ phosphors and Dy^{3+} (0.5 mol %) doped $LaPO_4$ phosphors and found to be 28 and 16 nm, respectively. It is also observed that no change in peak positions, but the intensity of the main peak is increased by 10%, maybe because of purity and complete single phase.

The examined SEM micrograph images reveal that the pure and Dy^{3+} (0.5 mol %) doped $LaPO_4$ phosphor samples originated from the solid microcrystalline structure with some agglomeration between the grains. The grains appeared agglomerated owing to the

high-temperature solid state synthesis. The average particle sizes of pure and Dy^{3+} (0.5 mol %) doped $LaPO_4$ phosphor is around 10 and 2 µm, respectively.

Finally, dysprosium (Dy^{3+}) (0.5 mol %) doped lanthanum phosphate ($LaPO_4$) phosphor under different excitations are synthesized by solid state reaction method; favorable emission in the deep blue region will make it one of the best candidates as a blue phosphor and are suitable for SSL technological applications in the LED devices.

Acknowledgment

One of the authors (CAR) is grateful for the financial support from the University Grant Commission (UGC), New Delhi, India, under Minor Research Project (MRP No: 4687/14-SERO/UGC). The author expresses his sincere thanks to K. V. R. M. Garu for providing Lab facility at M. S. University, Baroda. He is also very much thankful to the principal and management of the Bapatla College of Arts and Sciences, Bapatla for continuous encouragement during this project work.

References

1. M.Y. Guan, J.H. Sun, F.F. Tao, and Z. Xu, Cryst. Growth Des. **8**, 2694 (2008). https://doi.org/10.1021/cg070642z
2. Drug Delivery, ed. M. Schäfer- Korting (Springer-Verlag, Berlin Heidelberg, Germany2010).
3. S. Park, Z. Zhen, and D. H. Park, Mater. Lett. **649**, 1861 (2010). https://doi.org/10.1016/j.matlet.2010.05.017
4. N. O. Nunez, S. R. Livian, and M. Ocana, J. Coll. Interface Sci. **349**, 484 (2010). https://doi.org/10.1016/j.jcis.2010.05.079
5. P. Ghosh, J. Oliva, E. D. Rosa, K. K. Haldar, D. Solis, and A. Patra, J. Phys. Chem. C**112**, 9650 (2008). https://doi.org/10.1021/jp801978b
6. W. V. Schaik, S. Poort, G. Blasse, J. A. P. Omil, and S. B. Marquez, Chem. Mater. **6**, 755 (1994). https://doi.org/10.1021/cm00042a010
7. Z. Hou, L. Wang, H. Lian, R. Chai, C. Zhang, Z. Cheng, and J. Lia, J. Solid State Chem. **182,** 698 (2009). https://doi.org/10.1016/j.jssc.2008.12.021
8. S. Ding, D. Zhang, P. Wang, and J. Wang, Mater. Chem. Phys. **68**, 98 (2001).
9. Y. C. Kang, E. J. Kim, D. Y. Lee, and H. D. Park, J. Alloys Compd. **347**, 266 (2002). https://doi.org/10.1016/S0925-8388(02)00747-8
10. M. Yu, J. Lin, J. Fu, H. J. Zhang, and Y. C. Han, J. Mater. Chem. **13**, 1413 (2003). https://doi.org/10.1039/B302600K
11. G. C. Han, Y. H. Wang, C. F. Wu, and J. C. Zhang, Mater. Res. Bull. **44**, 2255 (2009), https://doi.org/10.1016/j.materresbull.2009.07.021
12. G. Phaomei, R. S. Ningthoujam, and W. R. Singh, Optical Mater. **32**, 616 (2010). https://doi.org/10.1016/j.optmat.2009.12.009
13. L. Yan, R.B. Yu, J. Chen, and X.R. Xing, Crystal. Growth Des **8**, 1474 (2008). https://doi.org/10.1021/cg800117v
14. Z. Lu, J. Zhou, A. Wang, N. Wang, and X. Yang, J. Mater. Chem. **21**, 4161 (2011). https://doi.org/10.1039/c0jm03299a
15. X. Chen, Z. Xia, M. Yi, X. Wu, and H. Xin, J. Phys. Chem. Solids **74**, 1439 (2013). https://doi.org/10.1016/j.jpcs.2013.05.002
16. P. Page andK. V. R. Murthy, Philosoph. Mag. Lett. **90**, 653 (2010). https://doi.org/10.1080/09500839.2010.491804

17. K. Suresh, K. V. R. Murthy, C.A. Rao, N. V. P. Rao and B. S. Rao, J. Lumin. **133**, 96 (2013). https://doi.org/10.1016/j.jlumin.2011.12.045
18. P. Nimishe and S. Dhoble, J. Adv. Mat. Lett. **2**, 358 (2011). https://doi.org/10.5185/amlett.2011.3073am2011
19. C. A. Rao, P. R. V. Nannapaneni, and K. V. R. Murthy, Adv. Mat. Lett. **4**, 207 (2013).
20. M. M. Yawalkar, G. D. Zade, V. Singh, and S. J. Dhoble, J. Mater. Sci. Mater. Electron. **28**, 180 (2017). https://doi.org/10.1007/s10854-016-5509-y
21. J. C. Wurst and J. A. Nelson, J. Am. Ceram. Soc. **55**, 109 (1972). https://doi.org/10.1111/j.1151-2916.1972.tb11224.x
22. K. Nakamoto, Infrared and Raman Spectra of Inorganic Coordination Compounds (Wiley, New York, 1986).
23. W. Kemp, Organic Spectroscopy (Macmillan, Hampshire, 1975. ISBN: S92K4 1991). https://doi.org/10.1007/978-1-349-15203-2
24. G. Vimal, K. P. Mani, P. R. Biju, C. Joseph, N. V. Unnikrishnan, and M. A. Ittyachen, Appl. Nanosci. **5**, 837 (2014). https://doi.org/10.1007/s13204-014-0375-5
25. B. Verma, R.N. Baghel, D. P. Bisen, N. Brahme, and V. Jena, Optical Mater. **118**, ID 111196 (2021). https://doi.org/10.1016/j.optmat.2021.111196
26. T. Gavrilović, J. Periša, J. Papan, K. Vuković, K. Smits, D. J. Jovanović, and M. D. Dramićanin, J. Lumin. **195**, 420 (2018). https://doi.org/10.1016/j.jlumin.2017.12.002
27. A. Ciric, S. Stojadinovíc, and M.D. Dramícanin, J. Lumin. **216**, ID 116749 (2019). https://doi.org/10.1016/j.jlumin.2019.116749
28. C. A. Rao, K. V. R. Murthy, Int. J. Innov. Sci. Res. Technol. **5** (2020).
29. Color Calculator Version 2, Software from Radiant Imaging, Inc. 2007.